



## Solvation of zero-valent metals in organic thin films

Amy V. Walker, Timothy B. Tighe, Michael D. Reinard, Brendan C. Haynie,  
David L. Allara, Nicholas Winograd \*

*Department of Chemistry, Pennsylvania State University, 184 Materials Research Institute Bldg., University Park, PA 16802, USA*

Received 29 July 2002; in final form 28 November 2002

### Abstract

Aluminum, copper and silver atoms are found to form a weakly solvated quasi-isotropic layer when vapor-deposited onto methoxy groups exposed at the surface of a hexadecanethiolate self-assembled monolayer on Au {111}. The nature of the interactions was revealed using SIMS, XPS and IRS, and supported by DFT calculations. This method complements 3D gas-phase cluster experiments by providing an approach for controlling solvation geometry and bonding via the molecular parameters of the monolayer. The results are discussed in terms of their applicability to the design of controlled interfaces, particularly metal contacts in molecular electronic devices.

© 2003 Elsevier Science B.V. All rights reserved.

### 1. Introduction

The interaction of metals with organic functional groups in thin films is important in a number of areas including organometallic chemistry, polymer chemistry and more recently to the growing field of molecular electronics. For example, the study of the reactivity of zero-valent metal atoms with molecular solvents comprises an important part of organometallic chemistry [1–6]. Details of the solvent–metal interactions are sparse since it is difficult to prepare solutions of isolated metal atoms in typical solvents, e.g., alkyl ethers. A limited amount of data is available from gas-

phase studies of solvated clusters and matrix isolation experiments [2–6]. Such experiments, while very informative in terms of solvation energetics and electron transfer properties, are not yet able to provide a complete picture of the structural geometry and bonding. The interaction of metals with polymer thin films also has been extensively examined at least in part due to the obvious technical applications. A central result of these studies on polymer films is the weakness of the interactions between various metal atoms, deposited from the vapor phase, and the polymer [7–9]. However, since it is difficult to ascertain the exact composition and structure of polymer surfaces, it has not yet been possible to elucidate the nature of the bonding that leads to such weak interactions.

In this Letter, we report on the use of self-assembled monolayers (SAMs) to reveal heretofore inaccessible details of the metal–organic functional

\* Corresponding author. Fax: +1-814-863-0618.

E-mail addresses: [dla3@psu.edu](mailto:dla3@psu.edu) (D.L. Allara), [nxw@psu.edu](mailto:nxw@psu.edu) (N. Winograd).

group interaction. These materials provide a unique template for these studies since it is possible to prepare surfaces with a wide variety of terminal group functionalities, composition and topographic configurations. The details of the bonding can be revealed using a combination of surface science probes. In this study we have employed time-of-flight secondary ion mass spectrometry (ToF SIMS), X-ray photoelectron spectroscopy (XPS) and infrared spectroscopy (IRS). The concept is illustrated by examining the interaction of Al, Cu and Ag atoms on the surface of a methoxy-terminated hexadecanethiolate SAM on gold, and is a model for the interaction of metal atoms with alkyl ether solvent molecules. The results show that these metal atoms interact with the methoxy terminal group forming a weakly solvating, quasi-isotropic layer. Concomitant theoretical calculations reveal the importance of orientational effects and provide additional insight into the detailed nature of the bonding. We recognize the applicability of this novel construct for the creation of highly controlled metal–organic interfaces. An important example is the control of the metal contacts in a variety of molecular electronic devices since the interaction is weak enough to allow the identity of the surface functional groups to be maintained, yet strong enough to provide an unimpeded path to electron flow.

## 2. Experimental

### 2.1. SAM preparation and analysis

The preparation and characterization of the types of SAMs used in this study has been described in detail previously [10,11]. Briefly, self-assembly of well-organized monolayers was achieved by immersing the Au substrates into millimolar solutions of the SAM molecules in absolute ethanol for  $\sim 2$  days at ambient temperature. The monolayer films were characterized with single wavelength ellipsometry, infrared spectroscopy and contact angle measurements to ensure that they were densely packed with clean surfaces.

In all cases, the metals (Al, Cu and Ag; Goodfellow, R.D. Mathis, Alfa Aesar  $\geq 99.995\%$ ) were

thermally evaporated at a rate of  $\sim 0.15$  atoms  $\text{nm}^{-2} \text{s}^{-1}$  as measured by a quartz crystal microbalance (QCM). Samples were kept in vacuum continuously during deposition and analysis.

The ToF SIMS analyses were performed on a custom designed instrument as described previously [12]. Briefly, the instrument consists of a loadlock, a preparation chamber, a metal deposition chamber and the primary analysis chamber, each separated by a gate valve. The primary  $\text{Ga}^+$  ions were accelerated to 15 keV and contained in a 100 nm diameter probe beam which was rastered over a  $(106 \times 106) \mu\text{m}^2$  area during data acquisition. All spectra were acquired using a total ion dose of less than  $10^{11}$  ions  $\text{cm}^{-2}$ . Relative peak intensities are reproducible to within  $\pm 8\%$  from sample to sample and  $\pm 8\%$  from scan to scan.

Infrared analyses were performed on a Fourier transform instrument (Mattson Research Series 1000) fitted with custom in-house optics configured external to the instrument and designed for grazing incidence reflection of samples under vacuum [10]. A liquid nitrogen cooled MCT detector was used with an effective low frequency cutoff of  $\sim 750 \text{ cm}^{-1}$ .

The XPS analyses were performed on a spectrometer (Scienta ESCA 300) equipped with a monochromatic Al-K $\alpha$  source, as described in detail elsewhere [13,14]. A pass energy of 75 eV and an energy step of 0.05 eV was used for the analysis. The resulting full width at half maximum (FWHM) for Au 4f $_{7/2}$  is 0.52 eV. A binding energy of 84.00 eV for Au 4f $_{7/2}$  was used as a reference for all spectra.

### 2.2. *Ab initio* quantum calculations

Density functional theory (DFT) calculations were performed to provide estimates of the interactions of the metal atoms – Al, Cu and Ag – and the methoxy group of the SAM. Calculations were carried out using the algorithms available in the GAUSSIAN 98 Rev. A.9 program package [15].

Interactions between SAM terminal groups and metal atoms can range from Van der Waals to weakly electrostatic to covalent [16]. To accurately determine these binding energies, small model systems were chosen to allow the use of larger

basis sets and various different starting geometries which would prove too computationally expensive if the entire alkanethiolate complex was used. Therefore the calculations were carried out on the simple isolated systems  $M + \text{CH}_3\text{OCH}_3$  and  $\text{CH}_3\text{CH}_2\text{CH}_3$ , where  $M = \text{Al}$ ,  $\text{Cu}$  and  $\text{Ag}$ . The most extensive results were obtained for Al atom complexes since the smaller number of electrons in comparison to Cu, Ag and Au allowed the use of larger basis sets. Geometry optimizations for these Al model systems were performed at using the B3PW91 functional with the 6-311+G(2df,p) and the LANL2DZ basis sets. Aluminum interaction energies using the B3PW91/6-311+G(2df,p) level of theory compare well to those calculated for Al with water [17,18] and dimethyl ether [19] using MP, quadratic configuration interaction (QCI) and CC methodologies [17–19] and experimentally derived values [20,21]. The Au, Ag and Cu complexes were run solely at the B3PW91/LANL2DZ level since the heavier metals require the use of effective core potentials (ECPs) to reduce the computational cost of the large number of electrons present in each atom. The use of ECPs has been shown by several groups to compare well with full electron calculations in the case of several small Au-, Ag- and Cu-containing molecules [22,23]. The interaction energy of the model system with Al, Cu and Ag were determined by relative energy of the geometry-optimized complex with respect to the energies of the optimized components. Additionally, thermal and zero point energy corrections were obtained from frequency calculations.

### 2.3. Definition of deposited metal coverage

For ease in data analysis and interpretation, the deposited amounts were converted to coverage of metal atoms per SAM molecule, designated  $\theta_M$  ( $M = \text{Al}$ ,  $\text{Cu}$  and  $\text{Ag}$ ). The SAM molecular density is 4.6 molecules  $\text{nm}^{-2}$  in a well-formed alkanethiolate/Au {111} SAM [24]. Thus for  $\theta_M = 1.0$  there would be one metal atom deposited on average per SAM molecule. In all data analysis we assume that the sticking probability of the deposited metal atoms is unity on the SAM monolayer. We assume the sticking probability is near unity

based upon comparison to XPS metal intensities with expected values obtained from the QCM. Moreover, in the SIMS experiments, metal signals are observed synchronously with the onset of metal deposition.

### 3. Results and discussion

The terminal group interaction with deposited Ag observed by ToF SIMS, XPS and IRS are displayed in Fig. 1. Upon deposition of Ag from the vapor phase on the  $-\text{OCH}_3$ -terminated SAM, a portion of the Ag atoms are found to penetrate to the Au/S interface and the remainder interact with the methoxy terminal group. Penetration of the Al and Cu atoms to the Au/S interface is also observed. For Cu and Ag, metal atom penetration continues at all metal coverages, whereas for Al, penetration of the metal atoms ceases after a 1:1 Al:Au ratio is achieved [10,25]. Penetration is uniquely correlated with the appearance of  $\text{Au}_x\text{Metal}_y\text{S}_z$  cluster ions observed by SIMS [10,25]. In the positive ion SIMS spectrum, the intensity of the  $\text{AgOCH}_3^+$  ( $m/z = 138$ ) peak is shown for increasing values of  $\theta_{\text{Ag}}$  (Fig. 1a). No  $\text{Ag}_x\text{O}_y^\pm$  ions are observed.

Based on our previous work [26,27] with  $-\text{COOH}$  and  $-\text{CO}_2\text{CH}_3$ -terminated SAMs, the appearance of  $\text{AgOCH}_3^+$  but not  $\text{Ag}_x\text{O}_y^\pm$  ions indicates that the deposited Ag has not undergone an insertion reaction with  $-\text{OCH}_3$  to form Ag–O bonds but suggests that a weak organo-silver complex has formed. Furthermore, upon deposition of Al and Cu,  $\text{MOCH}_3^+$  ions rather than  $\text{M}_x\text{O}_y^\pm$  ions are observed, where  $M = \text{Al}$ ,  $\text{Cu}$ , indicating that for these metals weak organo-metallic complexes have also formed.

The C1s peaks from the XPS spectra at 286.8 and 284.9 eV are assigned to the  $-\text{CH}_2\text{OCH}_3$  C atoms and the  $-(\text{CH}_2)-$  alkyl chain, respectively, as shown in Fig. 1b. Upon deposition of Ag, the  $-\text{CH}_2\text{OCH}_3$  peak vanishes by  $\theta_{\text{Ag}} \leq 37$  Ag atoms/SAM molecule. At the same time, the  $-(\text{CH}_2)-$  C1s peak broadens and shifts to a slightly higher binding energy (285.3 eV). For Al, the  $-\text{CH}_2\text{OCH}_3$  peak also disappears by  $\theta_{\text{Al}} \leq 1.3$  Al atoms/SAM molecule. These data indicate that on average

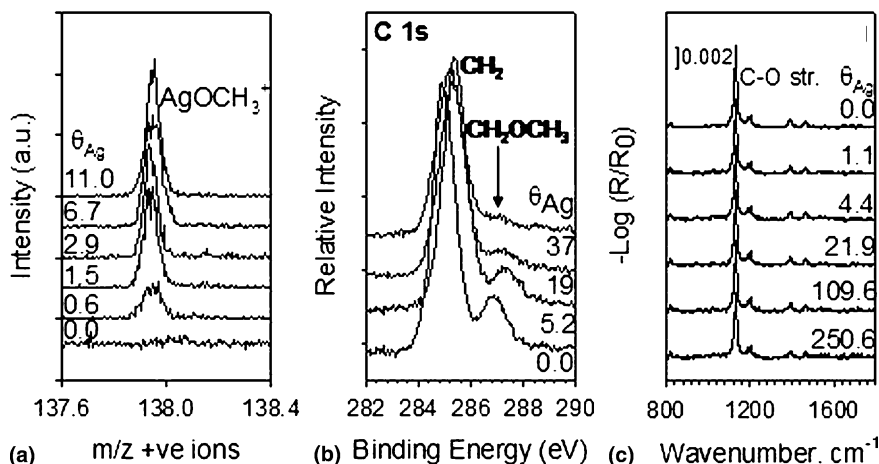


Fig. 1. (a) High mass resolution positive ion SIMS spectra of  $\text{AgOCH}_3^+$  fragments, nominal mass 138 Da. (b) XPS spectrum of C1s region of methoxy-terminated SAM upon deposition of Ag. (c) Low frequency IRS spectra of the methoxy-terminated SAM upon deposition of Ag.  $\theta_{\text{Ag}}$  is defined as the number of deposited Ag atoms per SAM molecule. Samples were kept in vacuum continuously during deposition and analysis.

there is a  $\sim 1:1$  perturbing interaction between the metal and the  $-\text{OCH}_3$  group that shifts the  $-\text{CH}_2\text{OCH}_3$  binding energy to lower values merging it into the main  $-(\text{CH}_2)-$  C1s peak. Further evidence of the Ag and Al interaction with the terminal group is given by the O1s spectrum (data not shown).

Perhaps the clearest evidence for the absence of Ag insertion into the  $-\text{OCH}_3$  group is given by the nearly constant character of the C–O stretching mode at  $1132 \text{ cm}^{-1}$  in the IRS spectra at all Ag coverages (Fig. 1c). The  $\delta_{\text{CH}_3}$  ( $\text{CH}_3$  def.,  $1383 \text{ cm}^{-1}$ ) and  $\delta_{\text{CH}_2}$  ( $\text{CH}_2$  scissor,  $1468 \text{ cm}^{-1}$ ) modes are also virtually unaffected by the deposition of Ag atoms. Taken together, these data indicate that there is no significant chemical interaction between the deposited Ag and the  $-\text{OCH}_3$ -terminated SAM. Similar behavior is found for Cu and Al deposition. Moreover, an Al–O stretch in the vicinity of  $\sim 855 \text{ cm}^{-1}$  is not observed confirming that there has been no bond cleavage at the methoxy terminal group.

Hence, the experimental data point to the formation of a weak  $\text{M}\cdots\text{OCH}_3$  complex, where  $\text{M} = \text{Al}, \text{Cu}$  and  $\text{Ag}$ , and rule out insertion of the metal atom into the C–O bond. Note the subtlety of the interaction: weak enough to cause little disturbance of the C–O stretching mode but strong

enough to perturb the local electron density such that the C1s binding energy shifts to lower binding energies.

To further quantify the interaction quantum mechanical calculations of isolated model systems,  $\text{M} + \text{CH}_3\text{OCH}_3$  and  $\text{CH}_3\text{CH}_2\text{CH}_3$ , where  $\text{M} = \text{Al}, \text{Cu}$  and  $\text{Ag}$ , were performed. For Ag and Cu insertion into the C–O bond, the calculations fail to converge indicating that the structure is unstable. Moreover, insertion of Ag and Cu into the C–C bond is unstable by 142 and 49  $\text{kJ mol}^{-1}$ , respectively, and would not be observed, in agreement with our observations. In contrast, for the Al system, the lowest energy configuration,  $-272 \text{ kJ mol}^{-1}$ , is the *insertion* of the Al into the C–O bond with a secondary minimum,  $-90 \text{ kJ mol}^{-1}$ , for insertion into the C–C bond. Since neither of these processes is observed experimentally, we assume that the activation barriers are prohibitively high.

However, there are secondary energy minima for all these systems for the stabilization of the metal atom [10,25] adjacent to O by  $-33 \text{ kJ mol}^{-1}$  for Al,  $-34 \text{ kJ mol}^{-1}$  for Cu and  $-13 \text{ kJ mol}^{-1}$  for Ag whilst there is no preference for the metal atom to be isolated or adjacent to the hydrocarbon. Thus, there is a preference for the metal atoms to be located close to the O atom rather than the C atom of the methoxy group.

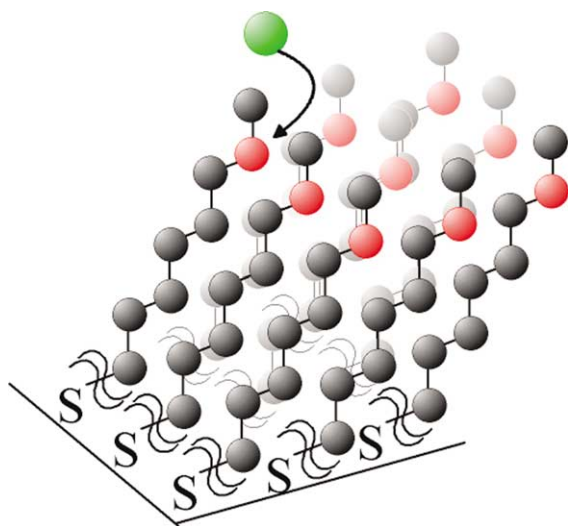


Fig. 2. Schematic illustration showing the steric hindrance of the metal oxygen atom. The metal atom is represented by the green sphere, oxygen atom is red and hydrocarbon moieties are black.

The minimum energy configuration for all the metal atoms is behind the O atom, away from the C–O bonds. Simple geometric considerations for the interaction of the SAM with the metal atom (Fig. 2) show that the isolated atom geometry will be unfavorable due to steric hindrances at the SAM/vacuum interface. While a small fraction of the methoxy groups may be able to reorient to allow ideal metal–oxygen interactions, most  $-\text{OCH}_3$  groups will not due to intermolecular repulsion forces. Thus we expect that the average stabilization energy per metal atom will be significantly reduced in the SAM case relative to the isolated system. This is in qualitative agreement with the observed behavior of the C–O stretch mode, which remains essentially unchanged upon metal deposition.

At room temperature, the methoxy group has a large number of configurations due to the low rotational energy barriers of the alkyl C–O bond relative to the C–C bond. There will be a wide range of configurations of metal atoms analogous to a weakly solvating, quasi-isotropic layer. We therefore view the interaction between these Al, Cu or Ag atoms and the methoxy terminal group as a ‘solvation’ rather than a complexation with a

directed interaction and a specific geometry. These experiments complement studies of solvation and electron transfer reactions of metal atoms with gas-phase molecules and clusters. In our experiments, whilst the underlying metal atom–molecular group interactions remain the same, the reaction is constrained to a quasi-planar configuration compared to the 3D geometry in the gas-phase experiment.

The ability to have such fine control of bonding interactions at metal–organic interfaces has important applications in the fabrication and design of top metal contacts for molecular electronics. In these applications, the fine control of metal–molecule bonding, ranging from no electronic overlap of states to complete chemical degradation, is critical in optimizing device performance [28].

#### 4. Conclusions

We have shown that with multiple surface science techniques, metal deposition on SAMS reveals the presence of weak metal–organic group interactions with high sensitivity. By constraining the interaction to a quasi-planar configuration, rather than 3D geometry in a gas-phase experiment, we are able to exploit properties such as steric hindrance, in addition to metal reactivity, and thus tune the properties of the metal–SAM system. This strategy has allowed us to observe solvation states for a number of metals in a controlled steric environment and points to new applications for these types of systems from designing new metallic contacts for organic electronic devices to catalysis.

#### Acknowledgements

The authors acknowledge financial support from the Office of Naval Research and the National Science Foundation.

#### References

- [1] K.J. Klabunde, in: R.A. Abramovitch (Ed.), *Reactive Intermediates*, vol. 1, Plenum Press, New York, 1980.

- [2] P. Kasai, *J. Phys. Chem. A* 106 (2002) 83.
- [3] D.B. Pederson, M.Z. Zgierski, S. Anderson, D.B. Rayner, B. Simard, S. Li, D.-S. Yang, *J. Phys. Chem. A* 105 (2001) 11462.
- [4] C.P. Schulz, C. Nitsch, *J. Chem. Phys.* 107 (1997) 9794.
- [5] J.J. Carroll, J.C. Weisshaar, *J. Phys. Chem.* 100 (1996) 12355.
- [6] P.A. Willis, H.U. Stauffer, R.Z. Hinrichs, H.F. Davis, *J. Chem. Phys.* 108 (1998) 2665.
- [7] J.J. Pireaux, *Syn. Met.* 67 (1994) 39.
- [8] T. Strunksus, M. Grunze, G. Kochendoerfer, Ch. Wöll, *Langmuir* 12 (1996) 2712.
- [9] F. Faupel, R. Willecke, A. Thran, *Mater. Sci. Eng. R* 22 (1998) 1.
- [10] G.L. Fisher, A.V. Walker, A.E. Hooper, T.B. Tighe, K.B. Bahnck, H.T. Skriba, M.D. Reinard, B.C. Haynie, R.L. Opila, N. Winograd, D.L. Allara, *J. Am. Chem. Soc.* 124 (2002) 5528.
- [11] P.E. Laibinis, C.D. Bain, R.G. Nuzzo, G.M. Whitesides, *J. Phys. Chem.* 99 (1995) 7663.
- [12] R.M. Braun, P. Blenkinsopp, S.J. Mullock, C. Corlett, K.F. Willey, J.C. Vickerman, N. Winograd, *Rapid Commun. Mass. Spectrom.* 12 (1998) 1246.
- [13] G. Beamson, D. Briggs, S.F. Davies, I.W. Fletcher, D.T. Clark, J. Howard, U. Gelius, B. Wannberg, P. Balzer, *Surf. Interface Anal.* 15 (1990) 541.
- [14] U. Gelius, B. Wannberg, P. Baltzer, H. Fellnerfeldegg, G. Carlsson, C.G. Johansson, J. Larsson, P. Munger, G. Vegerfors, *J. Electron Spectrosc. Relat. Phenom.* 52 (1990) 747.
- [15] M.J. Frisch et al., *GAUSSIAN 98*, Revision A.9, Gaussian Inc., Pittsburgh, PA, 1998.
- [16] S. Sakai, *J. Phys. Chem.* 96 (1992) 8369.
- [17] S. Sakai, *J. Phys. Chem.* 97 (1993) 8917.
- [18] J.M. Parnis, S.A. Mitchell, D.M. Rayner, P.A. Hackett, *J. Phys. Chem.* 92 (1988) 3869.
- [19] F.S. Legge, G.L. Nyberg, J.B. Peel, *J. Phys. Chem. A* 105 (2001) 7905.
- [20] J.M. Seminario, A.G. Zacarias, J.M. Tour, *J. Phys. Chem. A* 103 (1999) 7883.
- [21] J.M. Seminario, A.G. Zacarias, J.M. Tour, *J. Am. Chem. Soc.* 121 (1999) 411.
- [22] D.B. Pedersen, M.Z. Zgierski, S. Anderson, D.M. Rayner, B. Simard, *J. Phys. Chem. A* 105 (2001) 11462.
- [23] T. Fängström, S. Lunell, P.H. Kasai, L.A. Eriksson, *J. Phys. Chem. A* 102 (1998) 1005.
- [24] L.H. Dubois, R.G. Nuzzo, *Annu. Rev. Phys. Chem.* 43 (1992) 437.
- [25] A.V. Walker, T.B. Tighe, O. Cabarcos, M.D. Reinard, L. Dake, B.C. Haynie, D.L. Allara, N. Winograd, in preparation.
- [26] A. Hooper, G.L. Fisher, K. Konstadinidia, D. Jung, H. Nguyen, R. Opila, R.W. Collins, N. Winograd, D.L. Allara, *J. Am. Chem. Soc.* 121 (1999) 8052.
- [27] G.L. Fisher, A.E. Hooper, R.L. Opila, D.L. Allara, N. Winograd, *J. Phys. Chem. B* 104 (2000) 3267.
- [28] D.L. Allara, T.D. Dunbar, P.S. Weiss, L.A. Bumm, M.T. Cygan, J.M. Tour, W.A. Reinert, Y. Yao, M. Kozaki, L. Jones II, *Ann. NY Acad. Sci.* 852 (1998) 349.